



Electrostatic control over polarized currents through the spin-orbital Kondo effect

C. A. Büsser,¹ A. E. Feiguin,¹ and G. B. Martins^{2,*}

¹*Department of Physics and Astronomy, University of Wyoming, Laramie, Wyoming 82071, USA*

²*Department of Physics, Oakland University, Rochester, Michigan 48309, USA*

(Received 8 May 2012; published 28 June 2012)

Numerical calculations indicate that by suitably controlling the individual gate voltages of a capacitively coupled parallel double quantum dot, with each quantum dot coupled to one of two independent nonmagnetic channels, this system can be set into a spin-orbital Kondo state by applying a magnetic field. This Kondo regime, closely related to the SU(4) Kondo, flips spin from 1 to 0 through cotunneling processes that generate almost totally spin-polarized currents with opposite spin orientation along the two channels. Moreover, by appropriately changing the gate voltages of both quantum dots, one can simultaneously flip the spin polarization of the currents in each channel. As a similar zero magnetic field Kondo effect has been recently observed by Okazaki *et al.* [*Phys. Rev. B* **84**, 161305(R) (2011)], we analyze a range of magnetic field values where this polarization effect seems robust, suggesting that the setup may be used as an efficient bipolar spin filter, which can generate electrostatically reversible spatially separated spin currents with opposite polarizations.

DOI: 10.1103/PhysRevB.85.241310

PACS number(s): 72.15.Qm, 72.25.-b, 73.63.Kv, 85.75.Hh

Introduction. Traditional spintronic devices rely on the use of ferromagnetic source and drain leads to produce and detect polarized spin currents, like, for example, the Datta-Das spin field-effect transistor.¹ More recently, the manipulation of single spins has become one of the paradigms for quantum information.² To achieve easier integration with current technology, the use of semiconducting lateral single quantum dots (QDs) has been suggested as a means to produce spin filtering and spin memory devices,³ which can be controlled through the use of electrostatic gates, without the need of ferromagnetic contacts⁴ or highly inhomogeneous static magnetic fields or ac fields. Its experimental realization,⁵ using a single QD and a large magnetic field to produce a *bipolar* electrically tunable spin filter, has spurred a multitude of proposals, e.g., two QDs embedded in an Aharonov-Bohm ring,⁶ a double QD (DQD) in parallel,⁷ or in a T-shape geometry,⁸ to cite a few. More related to the results presented here, Borda *et al.*⁹ suggested the possibility of spin filtering in a DQD device at quarter filling, by exploiting spin and orbital degrees of freedom simultaneously through an SU(4) Kondo state. Right after that, Feinberg and Simon,¹⁰ by extending the ideas described in Ref. 9 to a similar DQD device, suggested the interesting possibility of a “Stern-Gerlach” spin filter effect at *half-filling*. In this work we use two fully independent channels, and present detailed numerical results confirming the high efficiency of the spin filtering effect and suggest experimental ways of observing it.

The utilization of the Kondo effect¹¹ in a single QD¹² has the potential to add an extra dimension to spintronics, as now the localized moment in a QD participates in a many-body state that may provide new functionalities to spintronic devices.¹³ More complex Kondo-like regimes, like the so-called SU(4) Kondo state,^{14,15} may provide even additional latitude to create, manipulate, and explore spintronic devices using QDs. In this work, we extend a recently observed variant of the SU(4) Kondo effect¹⁶ (dubbed the spin-orbital Kondo effect) to propose a device based on a capacitively coupled parallel DQD which, when in the Kondo regime (through the application of a magnetic field—see below), functions as a *bipolar*

spin filter that can produce currents with opposite polarities *simultaneously* (one in each channel of the DQD system). In addition, their polarities can be reversed by tuning the gate voltages of the QDs, i.e., the proposed bipolar spin filter is *electrically* tunable. As mentioned above, a similar device had been suggested before.¹⁰ Here, we provide extensive numerical results to stimulate experimental groups to try and observe this effect.

Device and Hamiltonian. The proposed setup is that of capacitively coupled parallel DQDs^{16,17} connected to *completely* independent metallic leads [see Fig. 1(a)].¹⁸ Through an even-odd transformation, two leads decouple from the DQD and the system is reduced to that shown in Fig. 1(b). Note that this transformation does not involve the QDs, therefore the interacting part of the Hamiltonian [(Eq. (2) below] remains unchanged. Then, the two-impurity Anderson Hamiltonian modeling our system is

$$H_{\text{tot}} = H_{\text{DQD}} + H_{\text{band}} + H_{\text{hyb}}, \quad (1)$$

$$H_{\text{DQD}} = \sum_{\lambda=1,2;\sigma} \left[\frac{U}{2} n_{\lambda\sigma} n_{\lambda\bar{\sigma}} + (V_{g\lambda} - \sigma H) n_{\lambda\sigma} \right] + U' \sum_{\sigma\sigma'} n_{1\sigma} n_{2\sigma'}, \quad (2)$$

$$H_{\text{band}} = t \sum_{\lambda=1,2} \sum_{i=1;\sigma}^{\infty} (c_{\lambda i\sigma}^{\dagger} c_{\lambda i+1\sigma} + \text{H.c.}), \quad (3)$$

$$H_{\text{hyb}} = \sum_{\sigma;\lambda=1,2} t_{\lambda} [d_{\lambda\sigma}^{\dagger} c_{\lambda 1\sigma} + \text{H.c.}]. \quad (4)$$

The operator $d_{\lambda\sigma}^{\dagger}$ ($d_{\lambda\sigma}$) creates (destroys) an electron in QD $\lambda = 1, 2$ with spin $\sigma = \pm$, while operator $c_{\lambda i\sigma}^{\dagger}$ ($c_{\lambda i+1\sigma}$) does the same at site i ($i + 1$) in a noninteracting semi-infinite chain $\lambda = 1, 2$; $n_{\lambda\sigma} = d_{\lambda\sigma}^{\dagger} d_{\lambda\sigma}$ is the charge per spin at each QD, and both QDs have the same charging energy U . We include the effect of a magnetic field H acting just on the QDs,³ and coupling just to the spin degree of freedom.¹⁹ For simplicity, we take the hybridization parameters $t_1 = t_2 = t'$. It is important to note that, contrary to Ref. 10, the *only*

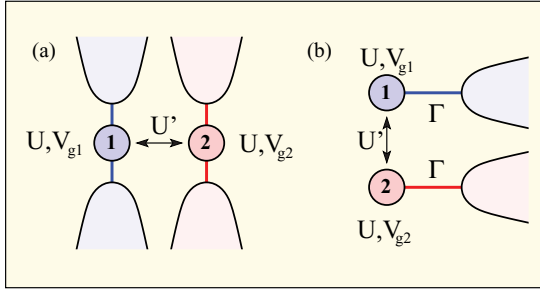


FIG. 1. (Color online) (a) DQD connected to four metallic leads so that conductance through them can be measured *independently*. The QDs are subjected to an inter-(intra-)QD Coulomb repulsion U' (U). (b) After an even-odd transformation, two of the leads decouple and the system is reduced to just two leads coupled *only* through U' .

interaction between electrons in different channels $\lambda = 1, 2$ is the interdot capacitive coupling U' . Finally, as our setup consists of semiconducting lateral QDs, each of them can have different gate potentials V_{g1} and V_{g2} ,^{16,18} and we will concentrate on the experimentally relevant regime $U'/U < 1.0$ [the so-called $SU(2) \otimes SU(2)$ regime].¹⁴ All results shown were calculated using U as our unit of energy. The width of the one-body resonance for each QD is given by $\Gamma = \pi t^2 \rho_0(E_F)$, where $\rho_0(E_F)$ is the density of states of the leads at the Fermi energy E_F . Throughout the paper $t = 1.0$ and all the other parameter values are indicated in the figures or in the text.

This model has been studied extensively in previous works, and it is well known that for $U'/U = 1.0$ and zero-field it has an $SU(4)$ Kondo fixed point¹⁴, experimentally observed in Refs. 20 and 21. Here, we want to address a completely different regime, although we will also show that our density-matrix renormalization-group (DMRG)²² calculations faithfully describe the $SU(4)$ Kondo regime as well.

Density matrix elements. The results presented in this work were calculated using the DMRG²³ and the Friedel sum rule (FSR).^{11,24–26} The validity of the FSR for the system studied here is discussed in the supplemental material.²⁷ In order to characterize and identify different regimes, we use the reduced density-matrix elements (DMEs), calculated with the DMRG. The ground-state wave function can be written as

$$|\Psi_0\rangle = \sum_{\gamma,\delta} \psi_{\gamma,\delta} |\gamma\rangle |\delta\rangle, \quad (5)$$

where γ stands for the 16 possible DQD configurations (0-0, σ -0, 0 - σ , σ - σ' , 2-0, 0-2, σ -2, 2- σ , and 2-2), while δ represents the states associated with the Fermi sea. Summing over the band states δ we obtain the weight projection of the different DQD configurations in the ground state,

$$\rho_{\gamma,\gamma'} = \sum_{\delta} \psi_{\gamma,\delta} \psi_{\gamma',\delta}^*. \quad (6)$$

As will be shown in Fig. 4, the diagonal DME can be used as a “proxy order parameter” for the typical correlations that characterize a many-body state like, for example, the Kondo state. This is very useful in the case of an unusual (or exotic) Kondo effect, where it may not be clear at first what the relevant correlations are that one should look for (from now

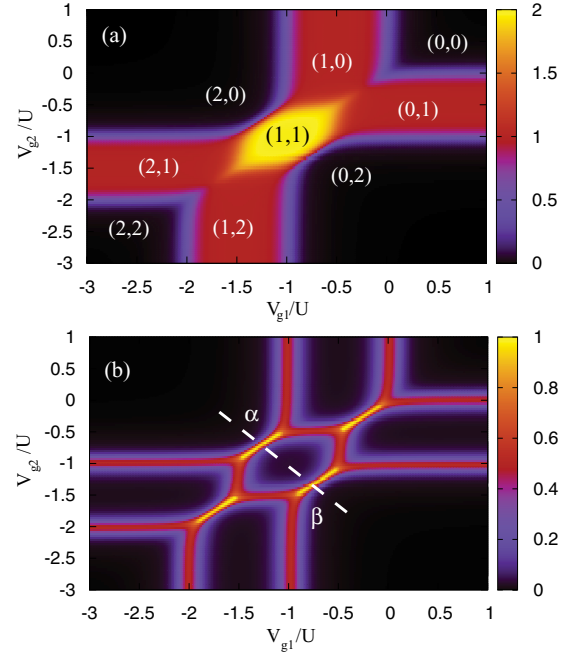


FIG. 2. (Color online) Conductance (in units of G_0) for $U' = 0.5$, $\Gamma = 0.02$, $H = 0.0$ (a) and $H = 0.05$ (b). (n_1, n_2) specifies the occupancies of each QD [same values apply to (b)]. (b) $H = 0.05$ suppresses the spin Kondo effect (note that color scales in each panel are different). We show that the bright (yellow) lines intercepted by the (white) dashed line, where $G = G_0$, correspond to a peculiar Kondo effect. Points α and β are discussed in detail in Figs. 3 and 4.

on we generally refer to the *diagonal* matrix elements as DME weight, or simply DME).

Numerical results. Figure 2(a) shows the conductance $G = G_1 + G_2$ ($G_{1,2}$ is the conductance for each channel) obtained through the FSR²⁷ in the V_{g1} - V_{g2} plane for $U' = 0.5$ at zero magnetic field. The different QD occupancies are indicated by

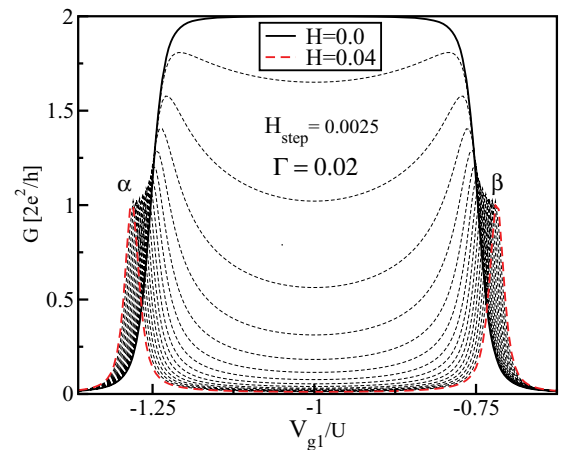


FIG. 3. (Color online) Effect of magnetic field over conductance along the (white) dashed line in Fig. 2(b). $U' = 0.5$, and $\Gamma = 0.02$, $0.0 \leq H \leq 0.04$ (field increases in steps of 0.0025). Half filling conductance (around $V_{g1} \sim -1.0$) in the $SU(2) \otimes SU(2)$ regime is suppressed faster than in the $SU(4)$ regime (not shown). The dashed (red) line ($H = 0.04$) reaches unitary conductance $G = G_0$ at values of V_{g1} corresponding to the points α and β in Fig. 2(b).

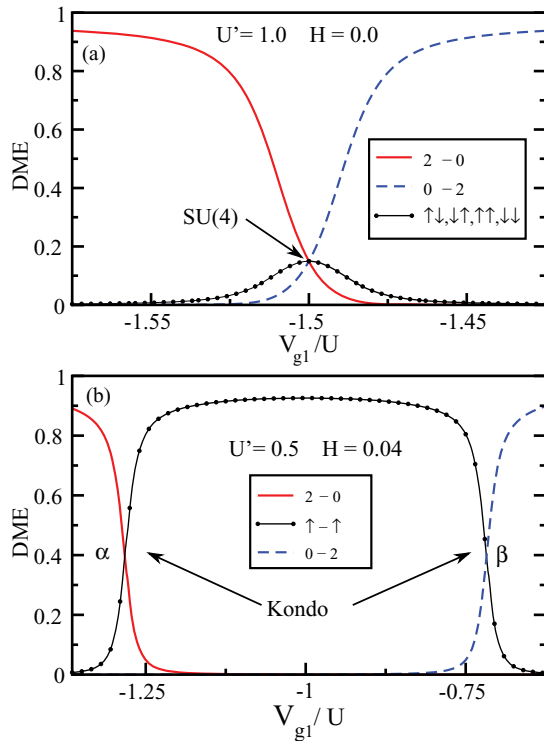


FIG. 4. (Color online) (a) DME vs V_{g1} for $V_{g2} = -V_{g1} - (1 + 2U')$, $\Gamma = 0.02$, $U' = 1.0$, and $H = 0.0$. At the p - h symmetric point ($V_{g1}/U = -1.5$), we have a half filling $SU(4)$ Kondo regime, characterized by the entanglement of spin and “orbital” degrees of freedom, translated here into the equality of all the two-electron DME DQD configurations at $V_{g1}/U = -1.5$. (b) Same as in (a), but now for $U' = 0.5$ [$SU(2) \otimes SU(2)$ regime] and $H = 0.04$, corresponding to the situation shown for the (red) dashed curve in Fig. 3. Note that the DME of the spin configuration $\uparrow\text{-}\uparrow$ [(black) dotted curve] is the same as the orbital configuration 2-0 [(red) solid curve] for $V_{g1} = -1.29$ (α point), as well as for the configuration 0-2 [(blue) dashed curve] for $V_{g1} = -0.71$ (β point).

the notation (n_1, n_2) . In Fig. 2(b) we present the conductance results for finite field $H = 0.05$, where the suppression of spin $SU(2)$ Kondo in each channel can be clearly observed [color scales are not the same for panels (a) and (b)]. The (white) dashed line is the region of gate voltage variation in the V_{g1} - V_{g2} plane that interests us. It is parametrized by the expression $V_{g2} = -V_{g1} - (1 + 2U')$. Conductance results along this line for $0.0 \leq H \leq 0.04$ are shown in Fig. 3, where the (black) solid line shows results at zero magnetic field, with a well defined plateau around $V_{g1} = -1.0$ [it corresponds to a cross section of the bright (yellow) region in Fig. 2(a)]. As the field increases, in steps of $\Delta H = 0.025$ (dotted lines), the conductance at (and around) the particle-hole (p - h) symmetric point ($V_{g1} = -1.0$) is suppressed very quickly, while narrow peaks start to form close to the charge degeneracy points [(red) dashed line], denoted α [(2,0)-(1,1)] and β [(0,2)-(1,1)] points in Fig. 2(b), where $G = G_0$. Note that these peaks are narrow along the (white) dashed line in Fig. 2(b), but along the charge degeneracy lines [the diagonal (yellow) bright lines in Fig. 2(b)] they present a clear plateau structure.

Now, in Fig. 4 we present one of the central results in this work. As an illustration of the use of DMEs to trace

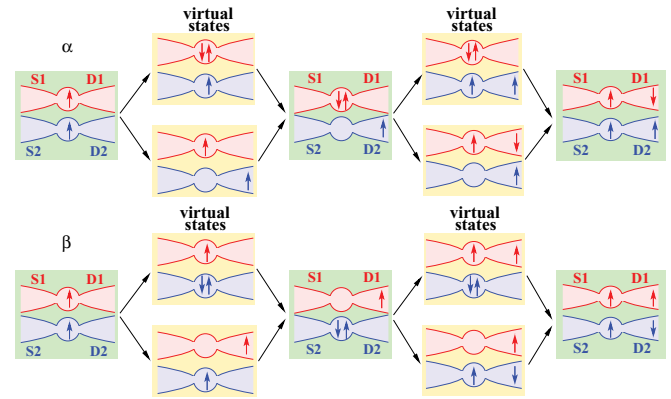


FIG. 5. (Color online) Top: Schematic representation of the four possible processes that flip the total spin from $S_z = 1$ to $S_z = 0$, and back to $S_z = 1$, when the singlet state is in channel 1 (α point). The net effect is the transport of a spin down (up) in channel 1 (2). The coherent superposition of these processes leads to Kondo screening of the pseudospin associated to the two degenerate states with $S_z = 1$ and $S_z = 0$, and the consequent generation of a spin down (up) current in channel 1 (2). Bottom: Equivalent processes for the configuration where the singlet state is in channel 2 (β point). In this case, the polarity of the currents in channels 1 and 2 (when compared to top panel) is reversed.

the possible existence of a Kondo regime, panel (a) shows the DME for half filling ($n_1 + n_2 = 2$) configurations of the DQD for $U' = 1.0$ and zero magnetic field [$SU(4)$ fixed point], as a function of V_{g1} for $V_{g2} = -V_{g1} - (1 + 2U')$ [equivalent to the dashed (white) line in Fig. 2(b), but for $U' = 1.0$ (see Supplemental Material²⁷)]. At the p - h symmetric point ($V_{g1} = V_{g2} = -U' - U/2 = -1.5$) in Fig. 4(a), i.e., at the half filled $SU(4)$ fixed point, one sees that the six possible two-electron configurations have all the same DME weight in the ground state, highlighting the fact that orbital and spin degrees of freedom are perfectly equivalent in the half filled $SU(4)$ Kondo state, i.e., spin and orbital degrees of freedom are *maximally* entangled.²¹ This result is well known, but it serves to illustrate the use of the DME calculation to “look for” possible Kondo states. This is what is done in panel (b), where we present the DME results for $U' = 0.5$ and finite field $H = 0.04$ [same parameters as the ones for the (red) dashed line in Fig. 3]. In this case, we have two different values of V_{g1} for which we have two half filling configurations with the same DME weight (the same V_{g1} values as the α and β points in Fig. 3). The crossing in the α (β) point in panel (b) is between configurations $\uparrow\text{-}\uparrow$ and 2-0 (0-2). The important fact to note is that *exactly* at these crossings $G = G_0$ (see Fig. 3), indicating the possibility of a Kondo effect.

Indeed, in Fig. 5 we show eight cotunneling processes (four in the upper panel and four in the lower) that shift the total S_z spin of the DQD from $S_z = 1$ to $S_z = 0$ (and vice versa). The top processes correspond to the degenerate states $\uparrow\text{-}\uparrow$ and 2-0 [α point in Fig. 4(b)], while the bottom processes correspond to the degenerate states $\uparrow\text{-}\uparrow$ and 0-2 (β point). The virtual states contain either one or three electrons. The remarkable fact about these cotunneling processes is that they generate spin polarized currents in each channel, with opposite polarizations. In addition, once one sweeps V_{g1} from α to β , the polarization

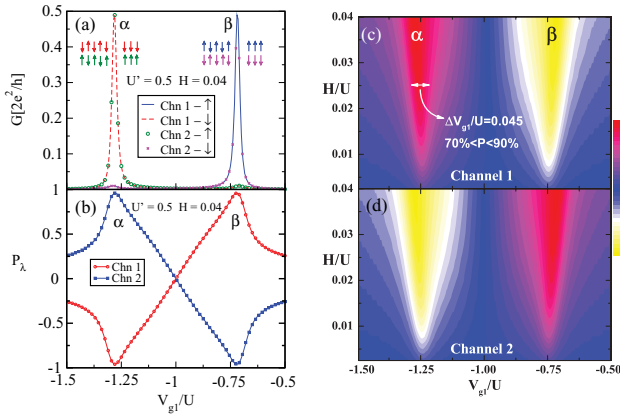


FIG. 6. (Color online) (a) Channel conductance per spin vs V_{g1} [same interval as in Figs. 3 and 4(b)], for $H = 0.04$ and $\Gamma = 0.2$: at point α channel 1 (2) is polarized down (up), and at point β channel 1 (2) is polarized up (down). (b) Polarization P_λ for each channel calculated using data from (a). (c), (d) Polarization vs V_{g1} ($0.0025 \leq H \leq 0.04$) for channels 1 and 2, respectively. Panel (c) also shows that for $H/U = 0.025$ there is a substantial range $\Delta V_{g1} \approx 0.045$ for which the spin polarization varies between $\approx 70\%$ and $\approx 90\%$, indicating that the effect should be experimentally observable.

direction of the *spin filtered* current in each right-side lead is reversed: \downarrow (\uparrow) and \uparrow (\downarrow) in channels 1 and 2, respectively, for the upper (lower) processes. Note that no other virtual states are connected (by t') to any of the degenerate states [$\uparrow\uparrow$ and $2-0$ ($0-2$)] in the α (β) point.²⁸ There are similarities between the Kondo effect described here and the one in Ref. 16: from the lower inset in their Fig. 2 we see that the magnetic field raises (lowers) the energy of the configuration $\downarrow\downarrow$ ($\uparrow\uparrow$), while maintaining the configurations $\uparrow\downarrow, 0, \uparrow\downarrow$, and $\downarrow\uparrow$ degenerate (to zero order in t'). By adjusting the gate potentials V_{g1} and V_{g2} , the configurations $\uparrow\downarrow, 0$ and $\uparrow\uparrow$ can be made degenerate (α point). Then, the coherent superposition of the cotunneling

processes in Fig. 5 give origin to the Kondo effect discussed here.²⁹

In Fig. 6(a), we show conductance per spin type as a function of V_{g1} [the same parameters as Fig. 3, (red) dashed curve] for channels 1 and 2 (see legend). These results confirm that the conductance at points α and β are almost perfectly polarized, in accordance with the cotunneling processes described in Fig. 5. Figure 6(b) shows the conductance polarization $P_\lambda = (G_{\lambda\uparrow} - G_{\lambda\downarrow}) / (G_{\lambda\uparrow} + G_{\lambda\downarrow})$ for channels $\lambda = 1, 2$. Panels (c) and (d) show polarization results for channels 1 and 2, respectively, for $0.0025 \leq H \leq 0.04$ [other parameters as in panels (a) and (b)]. The results clearly indicate that the polarization *effect* is robust and does not require a high value of magnetic field. Indeed, as indicated in Fig. 6(c), a polarization of almost 90% can be achieved for $H/U = 0.025$. Taking $U \approx 1.0$ meV for a GaAs QD¹⁸ results in $H \lesssim 1.0T$ around the α point. As indicated by the double-head white arrow in Fig. 6(c), a range of $\Delta V_{g1} \approx 0.045$, at $H/U = 0.025$, has a polarization varying from $\approx 70\%$ to $\approx 90\%$. This indicates that there is enough range in the parameter space to allow for experimental observation of very high polarizations without the need of very high magnetic fields.

Conclusions. In summary, we have presented a peculiar Kondo effect involving a capacitively coupled parallel DQD, connected to two independent channels. To achieve this effect it is necessary to apply a moderate magnetic field and adjust the gate potential of each QD to take the DQD to a half filling charge degeneracy point. The cotunneling processes in this Kondo effect are such that spin polarized currents are generated in each channel, with opposite polarities. The results in Fig. 6 indicate that the effect should be experimentally observable.

Acknowledgments. The authors acknowledge very fruitful conversations with S. Amasha, D. Goldhaber-Gordon, A. Keller, and E. Vernek. G.B.M. acknowledges financial support by NSF under Grants No. DMR-1107994 and DMR-0710529, and A.E.F. under Grant No. DMR-0955707.

*Corresponding author: martins@oakland.edu

¹S. Datta and B. Das, *Appl. Phys. Lett.* **56**, 665 (1990).

²F. Chi and Q.-F. Sun, *Phys. Rev. B* **81**, 075310 (2010); P. Trocha, *Solid State Commun.* **151**, 725 (2011), and references therein.

³P. Recher, E. V. Sukhorukov, and D. Loss, *Phys. Rev. Lett.* **85**, 1962 (2000).

⁴S. Csonka, I. Weymann, and G. Zarand, *Nanoscale* **4**, 3635 (2012).

⁵R. Hanson, L. M. K. Vandersypen, L. H. Willems vanBeveren, J. M. Elzerman, I. T. Vink, and L. P. Kouwenhoven, *Phys. Rev. B* **70**, 241304(R) (2004).

⁶E. R. Hedin and Y. S. Joe, *J. Appl. Phys.* **110**, 026107 (2011).

⁷J. P. Dahlhaus, S. Maier, and A. Komnik, *Phys. Rev. B* **81**, 075110 (2010).

⁸F. Mireles, S. E. Ulloa, F. Rojas, and E. Cota, *Appl. Phys. Lett.* **88**, 093118 (2006).

⁹L. Borda, G. Zaránd, W. Hofstetter, B. I. Halperin, and J. von Delft, *Phys. Rev. Lett.* **90**, 026602 (2003).

¹⁰D. Feinberg and P. Simon, *Appl. Phys. Lett.* **85**, 1846 (2004).

¹¹A. C. Hewson, *The Kondo Problem to Heavy Fermions* (Cambridge University Press, Cambridge, England, 1993).

¹²D. Goldhaber-Gordon, H. Shtrikman, D. Mahalu, D. Abusch-Magder, U. Meirav, and M. A. Kastner, *Nature (London)* **391**, 156 (1998).

¹³J. R. Hauptmann, J. Paaske, and P. E. Lindelof, *Nat. Phys.* **4**, 373 (2008).

¹⁴M. R. Galpin, D. E. Logan, and H. R. Krishnamurthy, *Phys. Rev. Lett.* **94**, 186406 (2005); *J. Phys.: Condens. Matter* **18**, 6545 (2006); **18**, 6571 (2006), and references therein. See also F. B. Anders, D. E. Logan, M. R. Galpin, and G. Finkelstein, *Phys. Rev. Lett.* **100**, 086809 (2008).

¹⁵C. A. Büsser and G. B. Martins, *Phys. Rev. B* **75**, 045406 (2007); M. Mizuno, E. H. Kim, and G. B. Martins, *J. Phys.: Condens. Matter* **21**, 292203 (2009).

- ¹⁶Y. Okazaki, S. Sasaki, and K. Muraki, *Phys. Rev. B* **84**, 161305(R) (2011).
- ¹⁷A. Hübner, K. Held, J. Weis, and K. v. Klitzing, *Phys. Rev. Lett.* **101**, 186804 (2008); P. Trocha, *Phys. Rev. B* **82**, 125323 (2010); G. C. Tettamanzi, J. Verduijn, G. P. Lansbergen, M. Blaauboer, M. J. Calderon, R. Aguado, and S. Rogge, *Phys. Rev. Lett.* **108**, 046803 (2012).
- ¹⁸S. Amasha, A. J. Keller, I. G. Rau, J. A. Katine, H. Shtrikman, and D. Goldhaber-Gordon (private communication).
- ¹⁹Note that the pseudospin operator associated to the orbital degree of freedom depends only on the total charge in each QD and thus does not couple to the magnetic field.
- ²⁰A. Makarovski, J. Liu, and G. Finkelstein, *Phys. Rev. Lett.* **99**, 066801 (2007).
- ²¹P. Jarillo-Herrero, J. Kong, H. S. J. van der Zant, C. Dekker, L. P. Kouwenhoven, and S. De Franceschi, *Nature (London)* **434**, 484 (2005).
- ²²S. R. White, *Phys. Rev. Lett.* **69**, 2863 (1992).
- ²³The DMRG calculations were done keeping typically between 600 and 1000 states, for clusters with up to 40 sites.
- ²⁴D. C. Langreth, *Phys. Rev.* **150**, 516 (1966).
- ²⁵M. R. Galpin, F. W. Jayatilaka, D. E. Logan, and F. B. Anders, *Phys. Rev. B* **81**, 075437 (2010).
- ²⁶L. Vaugier, A. A. Aligia, and A. M. Lobos, *Phys. Rev. B* **76**, 165112 (2007).
- ²⁷See Supplemental Material at <http://link.aps.org/supplemental/10.1103/PhysRevB.85.241310> for details of the Friedel Sum Rule calculations and examples of the use of the Density Matrix Elements.
- ²⁸For a discussion of the Kondo Hamiltonian associated to this effect, see Ref. 10, and for the hierarchical order of energy scales in a realistic setup, see Refs. 9 and 10.
- ²⁹Note that cotunneling processes also occur in the Coulomb blockade (CB) regime. What distinguishes these from the cotunneling processes in the Kondo effect is that the last are associated to an increase in spin fluctuations (which reach a maximum at the p - h point), while no increase in spin fluctuations occurs in the CB regime. Furthermore, the pseudospin fluctuations are *essential* to produce the particular spin polarization present in our results (see Fig. 5).